J|A|C|S COMMUNICATIONS

Published on Web 05/04/2010

Biomineralization-Assisted Ultrasensitive Detection of DNA

Xin Zhou, Sijing Xia, Zhiqiang Lu, Yuan Tian, Yishu Yan, and Jin Zhu*

Department of Polymer Science and Engineering, School of Chemistry and Chemical Engineering, State Key Laboratory of Coordination Chemistry, Nanjing National Laboratory of Microstructures, Nanjing University, Nanjing 210093, China

Received March 18, 2010; E-mail: jinz@nju.edu.cn

Biomineralization refers to the biologically controlled formation of mineral deposits.[1] The precision and quality showcased by the exquisite structures have prompted the investigation of functional attributes derived from these fascinating processes.[2−4] Indeed, remarkable mechanical,[2] magnetic,[3] and optical[4] properties have been identified to be integral to a diversity of stringently selected biogenic species. The advent of molecular biology[5] has further inspired the materials architecture control[6] through mechanistic insights into the underlying constituent components. In this regard, the continued exclusive dominance of function-oriented synthesis contrasts with the notable absence of diagnostics-targeted application, despite the fact that biomineralization is inherently a catalytic process. The dichotomy likely reflects the challenge involved in the integration of such a nature-derived strategy into a signal generation scheme. Indeed, inventive design of assay architectures,[7−9] key to the innovation in molecular diagnostics, often requires highly demanding eclectic efforts. Herein, we report on the utility of a biomineralization-assisted amplification (BMA) methodology for the highly sensitive and selective detection of DNA. Significantly, this strategy has allowed the achievement of 50 aM target identification (equivalent to ∼180 copies in the entire 6 μL sample) and single-base mismatch differentiation.

DNA detection has been the subject of intense interest[10] by virtue of its importance in clinical diagnostics, gene therapy, and forensic analysis. Traditional methods frequently require expensive instrumentation[11] and are therefore not suited for practice in numerous settings. Our approach to DNA detection is to implement a silica formation, biological amplification process into a chip-based, visual signal readout pathway (Figure 1). In particular, the BMA assay involves the utility of two types of gold nanoparticle (AuNP) probes. The first probe (AuNP-**S** probe) is a AuNP simultaneously functionalized with both target-recognition oligonucleotide (5′ HS-AAAAAAAAAAATCCTTATCAAT 3′, DNA **1**) and biomineralization-capable silicatein.[5a,b] The second probe (AuNP-**O** probe) is a monolayer-protected AuNP with an oligo(ethylene glycol) (OEG) derivative ($HS(CH_2CH_2O)_4CH_2COOH$,[12] molecule **2**) as the capping species. These two probes allow the detection of DNA, as illustrated in Figure 1, through a cascade signal amplification process: first, a transparent solid support surface modified with a capture oligonucleotide (5′ ATTTAACAATAATCCAAAAAAAAAA-SH 3′, DNA **4**) is used to hybridize with both target oligonucleotide (5′ GGATTATTGTTAAATATTGATAAGGAT 3′, DNA **3**)[7−9] and AuNP-**S** probe in a sandwich manner; second, silicatein on the AuNP-**S** surface catalyzes the synthesis of silica that enables the simultaneous entrapment of AuNP-**O** probe; and finally, selective deposition of silver metals[13] on both AuNP-**S** and AuNP-**O** probes furnishes the facile visualization of signal with high sensitivity.

Several distinguishing features of our BMA system deserve comments: (1) the biomineralization and followup processes are decoupled from the molecular binding event, thus potentially allowing for target identification beyond DNA; (2) the assay scheme is devoid of polymerase chain reaction (PCR) in the case of DNA detection, important for the elimination of drawbacks associated with this exponential duplication process (e.g., sensitivity to contamination); (3) as compared to the liquid product-based conventional enzymatic systems (e.g., enzyme-linked immunosorbent assay), the biomineralization-generated product is in the solid state format, rendering it compatible with the chip array platform; and (4) the probe fabrication relies on the utility of a AuNP as the carrier, thus avoiding the engagement of complex conjugation chemistry in the covalent bonding of target-recognition and signal-amplification units.

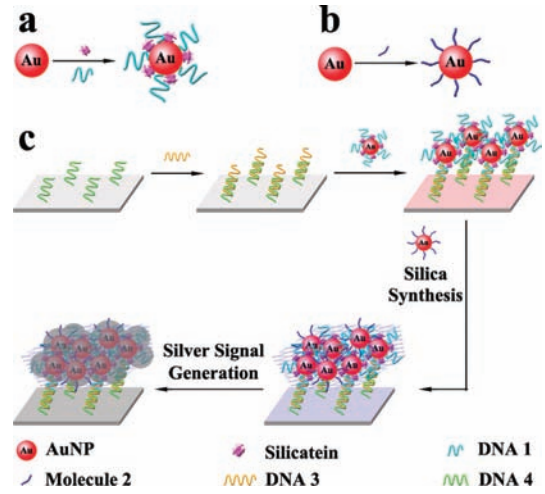

Figure 1. Schematic representation of the BMA strategy. (a) Fabrication of AuNP-**S** probe. AuNP-**S** probe is prepared through the one-pot sequential loading of silicatein and DNA **1** (5′ HS-AAAAAAAAAAATCCTTATCAAT 3′) onto AuNPs. (b) Fabrication of AuNP-**O** probe. AuNP-**O** probe is prepared through the loading of molecule **2** ($HS(CH_2CH_2O)_4CH_2COOH$) onto AuNPs. (c) DNA detection based on the BMA strategy. A glass slide modified with capture DNA **4** (5′ ATTTAACAATAATCCAAAAAAAAAA-SH 3′) is hybridized in a sandwich manner with target DNA **3** (5′ GGATTATTGTTAAATATTGATAAGGAT 3′) and AuNP-**S** probe; silicatein on the AuNP-**S** probe is then used to catalyze the synthesis of silica in the presence of AuNP-**O** probe; target DNA identification is achieved through the visual readout of silver signal generated through selective deposition on the AuNP-**S** and AuNP-**O** probes.

Silicateins are a collection of proteins (α, β, and γ subunits) isolated from the marine demosponge *T. aurantia*.[5a,b] Molecular cloning has enabled the production of recombinant silicatein α that is capable of promoting the formation of silica under physiological conditions. As such, silicatein with a N-terminal His tag was expressed from a plasmid, pET28a-Silicatein, in the *E. coli* strain BL21 (Figure S1). The biomineralization capability of the protein was confirmed with the colorimetric molybdate assay for the

 10.1021/ja102271r

produced silica (Figures S2−S5).[5b] AuNP-**S** probe (Figures S6 and S7) was then fabricated through the one-pot sequential loading of silcatein and DNA **1** onto citrate-stabilized AuNPs. With UV−vis extinction spectroscopy (Figure S8), gel electrophoresis (Figure S9), and fluorescence spectroscopy (Figure S10) as the quantification tools, the number of silicatein and DNA **1** on a single AuNP-**S** probe was calculated to be ∼5 and 37, respectively. Importantly, in the surface-confined state, neither the biomineralization capacity of silicatein (Figures S2 and S3) nor the hybridization competence of DNA **1** (Figure S11) is compromised. The synthesis of AuNP-**O** probe was carried out through direct incubation of citrate-stabilized AuNPs in an aqueous solution of molecule **2**. For AuNP-**O** probe, two defining characteristics render it extremely useful in our BMA assay: high stability under a plethora of conditions ensured by the combination of a protecting OEG unit and carboxylic acid group, and biological inertness due to the packing density and hydrophilicity feature of the flexible OEG chain.[14]

With AuNP-**S** and AuNP-**O** probes in hand, we next examined the feasibility of employing the BMA strategy for the detection of DNA. To this end, a glass slide was covalently modified with a capture strand DNA **4** through a bifunctional coupling reagent, succinimidyl 4-(*N*-maleimidomethyl)cyclohexane-1-carboxylate (SMCC).[8] At high target concentrations, the sandwich structure formed from DNA **4**, target **3**, and AuNP-**S** probe allowed the immobilization of AuNP-**S** probe onto the glass slide and direct visualization of the hybridization process (Figure 2). In the dehydrated state, the AuNP-**S**-loaded spot exhibits a blue-colored outlook, reflecting close-packing-conferred electronic coupling of AuNP-**S** probe. The color of the spot changes dramatically after the subsequent catalytic silica synthesis procedure in the presence of AuNP-**O** probe (Figure 2). The change in the color, an indication of variation of the surface plasmon resonance band, is most likely the result of alteration of the dielectric constant and loading density of AuNPs on the surface. To validate the hypothesis and probe the structural change, scanning electron microscopy (SEM) was used to monitor the state of the surface before and after the biomineralization step (Figure 3). Indeed, an extensive silica network was observed along with the pronounced increase of AuNP density, pointing toward the efficient entrapment of AuNP-**O** probe during the catalytic reaction. A negative control experiment in the absence of target DNA (Figure S12) provides evidence that nonspecific binding of AuNP probes is minimal under the conditions employed herein. In addition, target DNA-driven immobilization of AuNP-**S** probe and subsequent catalytic formation of silica were further supported by the energy-dispersive X-ray (EDX) spectroscopy observation of intense Si and Au signals on the solid support surface (Figure S13).

These promising results prompted us to investigate the utility of enzymatically immobilized AuNP-**O** probe, together with AuNP-**S** probe, as an intermediate mediator in a tandem reaction to orchestrate a final signal amplification process. A silver signal generated preferentially on AuNP probes[13] could be employed as such a tool to allow visual readout. Indeed, silver staining imparted a dark outlook upon the spot (Figure 2) and provided a convenient way to identify target DNA. Importantly, the silver signal produced on the glass slide with AuNP-**O** probe immobilized is more pronounced than that in the absence of such a probe (Figures 2 and S14), indicating the critical role played by the AuNP-**O** in the silver staining process. The rationale behind the phenomenon was investigated with SEM, which revealed the presence of highly intertwined silver networks for a sample with AuNP-**O** probe, as compared to the sparsely dispersed silver particles generated either without this probe (Figure S15) or directly on a AuNP-**S**-loaded

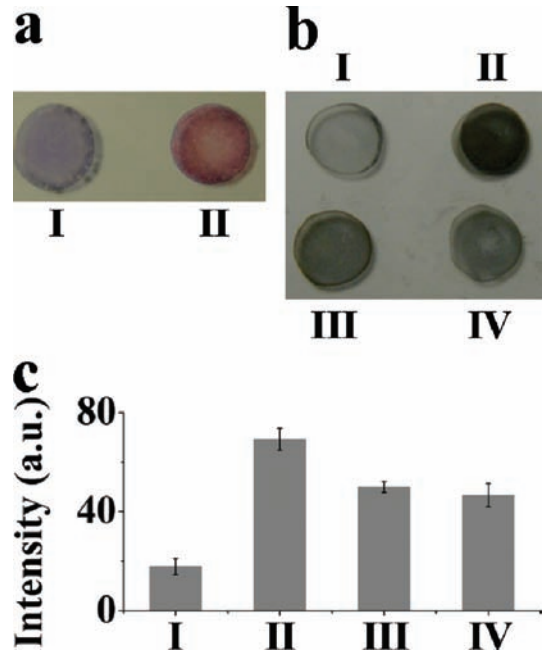

Figure 2. DNA detection based on the signal generation by the BMA method. (a) Macroscopic image of a DNA **4**-spotted glass slide after hybridizing with DNA **3** (1 μM) and AuNP-**S** probe (I) and further in silica formation process in the presence of AuNP-**O** probe (II). (b) Macroscopic image of a DNA **4**-spotted glass slide after hybridizing with 0 (I), 100 (II), 10 (III), and 1 (IV) fM DNA **3** and AuNP-**S** probe, silica formation process in the presence of AuNP-**O** probe, and silver staining step (18 °C, 3 min, twice). The dark spot generated on the hybridization site allows the visual identification of target DNA. (c) Quantification of signals generated in (b) through the measurement of grayscale image intensity of the spot with Adobe Photoshop. The image intensity obtained for the graph was calculated by subtracting the background value surrounding the spot from that in the spot.

surface (Figure 3). We reasoned that the more pronounced signal amplification can be translated into a more sensitive DNA detection scheme. Indeed, under unoptimized conditions, the silver signal could be resolved at a DNA concentration as low as 50 aM (∼180 molecules in 6 μL) with our BMA strategy (Figure 4). This detection capability represents a 3 orders of magnitude increase in the sensitivity over the previously reported scanometric method[13] that lacks the BMA step. In addition, the grayscale image intensity of the spot can be extracted with an image processing software such as Adobe Photoshop and could offer quantitative correlation with the target DNA concentration (Figure 2).

One prominent feature of using a AuNP probe is the ability to differentiate the perfect target from mismatched DNA due to the unique sharp melting transition of the dehybridization process.[13] The multiligand-derived cooperative behavior has further enabled the development of a salt-based stringency wash method for the selective denaturation of imperfect duplexes.[15,16] We opted for this strategy to inspect the selectivity of our BMA strategy by virtue of its elimination of the need for an on-chip temperature control. Initial examination of a highly mismatched DNA strand confirmed the ability to detect the perfect target through the performance of a salt stringency wash after the hybridization process (Figure S16). We have therefore proceeded to the more technically demanding single-base mismatch differentiation challenge. The detection of single-base mismatches is important for the routine screening of genetic mutations and diseases. Satisfactorily, the utility of heavily oligonucleotide-functionalized AuNP-**S** probe permits the discrimination of the perfect target from the one with a single-base mismatch (Figure S17).

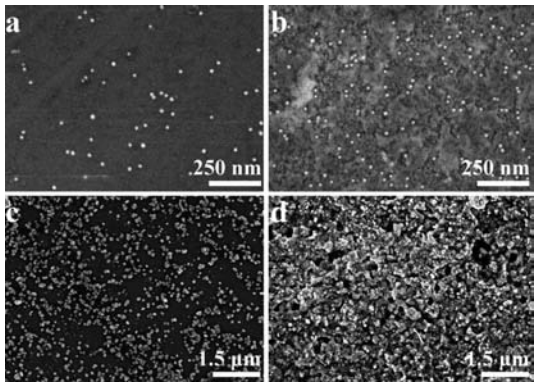

Figure 3. Characterization of the structural change on the solid support surface after the BMA process. (a) SEM micrograph of a DNA **4**-derivatized silicon wafer after hybridizing with DNA **3** (100 pM) and AuNP-**S** probe. (b) SEM micrograph of a silicon wafer identical to that in (a) after the silica formation process in the presence of AuNP-**O** probe. Extensive silica network, as well as pronounced increase in the AuNP density, could be observed. The number of countable AuNPs in (b) is 146, as compared to 59 in (a). A higher AuNP density translates into a more efficient silver deposition process. (c) SEM micrograph of a silicon wafer identical to that in (a) after the silver staining process (18 °C, 3 min). (d) SEM micrograph of a silicon wafer identical to that in (b) after the silver staining process (18 °C, 3 min). The formation of apparent intertwined silver network structure could be observed in (d), as compared to only the sparsely distributed particle structure in (c). The BMA strategy therefore offers a notable increase in the amount of silver metals that translates into higher signal intensity and assay sensitivity. Silicon wafer is used to replace the glass slide as a support for the purpose of SEM imaging due to its analogous surface chemistry, electrical conductivity, and smooth surface morphology.

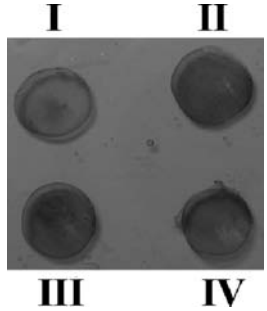

Figure 4. Detection limit for DNA under unoptimized conditions. Macroscopic image of a DNA **4**-spotted glass slide after hybridizing with 0 (I), 500 (II), 50 (III), and 10 (IV) aM DNA **3** and AuNP-**S** probe, silica formation process in the presence of AuNP-**O** probe, and silver staining step (18 °C, 3 min, twice). Repeated experiments demonstrated that signals could be reproducibly resolved at a DNA concentration as low as 50 aM.

For an enzymatic amplification-based diagnostic platform, a direct transformation of a labeled reactant into an amplified product with a readout signal could be an alternative to the BMA method developed herein. The elasticity and adaptability of silicatein on the substrate scope[5a] show promising feasibility in the implementation of such a straightforward scheme. Further, rational and combinatorial protein engineering technology should render it potentially viable to generate other types of signals (e.g., fluorescence) and develop diverse detection systems through silicatein variant-catalyzed reactions on desired functional group-modified substrates. Biomineralization has been a foremost tool in the materials science arena, and with the initial proof-of-concept demonstration provided herein, it is our belief that it will contribute tremendously to the revolution of molecular diagnostics technologies.

In summary, biomineralization has been employed as an effective tool to facilitate the detection of DNA. The distinctly staged yet sequentially coupled DNA hybridization and signal amplification processes ensure both high sensitivity and high selectivity. The system combines the instrument-free operation convenience with the extraordinary detection capability and is therefore ideally suited for highly demanding tests in resource-poor settings. Substitution of the DNA structures with other recognition moieties should allow the translation of the strategy to the assay of a broad range of targets of interest.

Acknowledgment. J.Z. acknowledges support from the National Natural Science Foundation of China (20604011, 20974044, 90923006), the National Basic Research Program of China (2007CB925103), and the Program for New Century Excellent Talents in University (NCET-06-0451).

Supporting Information Available: Experimental procedures, characterization of the probe, and DNA detection data. This material is available free of charge via the Internet at http://pubs.acs.org.

References

(1) (a) Douglas, T. *Science* **2003**, *299*, 1192–1193. (b) Wilt, F. H. *Dev. Biol.* **2005**, *280*, 15–25.
(2) (a) Meyer, M. A.; Chen, P.-Y.; Lin, A. Y.-M.; Seki, Y. *Prog. Mater. Sci.* **2008**, *53*, 1–206. (b) Mayer, G. *Science* **2005**, *310*, 1144–1147.
(3) Bazylinski, D. A.; Frankel, R. B. *Nat. Rev. Microbiol.* **2004**, *2*, 217–230.
(4) Sundar, V.; Yablon, A. D.; Grazul, J. L.; Ilan, M.; Aizenberg, J. *Nature* **2003**, *424*, 899–900.
(5) (a) Brutchey, R. L.; Morse, D. E. *Chem. Rev.* **2008**, *108*, 4519–4534. (b) Cha, J. N.; Shimizu, K.; Zhou, Y.; Christiansen, S. C.; Chmelka, B. F.; Stucky, G. D.; Morse, D. E. *Proc. Natl. Acad. Sci. U.S.A.* **1999**, *96*, 361–365. (c) Suzuki, M.; Saruwatari, K.; Kogure, T.; Yamamoto, Y.; Nishimura, T.; Kato, T.; Nagasawa, H. *Science* **2009**, *325*, 1388–1390. (d) Sumper, M.; Brunner, E. *ChemBioChem* **2008**, *9*, 1187–1194.
(6) (a) Sano, K.-I.; Yoshii, S.; Yamashita, I.; Shiba, K. *Nano Lett.* **2007**, *7*, 3200–3202. (b) Yamashita, I. *J. Mater. Chem.* **2008**, *18*, 3813–3820.
(7) Zhou, X.; Cao, P.; Tian, Y.; Zhu, J. *J. Am. Chem. Soc.* **2010**, *132*, 4161–4168.
(8) Hong, M.; Zhou, X.; Lu, Z.; Zhu, J. *Angew. Chem., Int. Ed.* **2009**, *48*, 9503–9506.
(9) Qiu, F.; Jiang, D.; Ding, Y.; Zhu, J.; Huang, L. L. *Angew. Chem., Int. Ed.* **2008**, *47*, 5009–5012.
(10) Sassolas, A.; Leca-Bouvier, B. D.; Blum, L. J. *Chem. Rev.* **2008**, *108*, 109–139.
(11) Makrigiorgos, G. M.; Chakrabarti, S.; Zhang, Y.; Kaur, M.; Price, B. D. *Nat. Biotechnol.* **2002**, *20*, 936–939.
(12) Lu, Z.; Shu, X.; Zhang, K.; Zhu, J. *J. Phys. Chem. C* **2009**, *113*, 12950–12953.
(13) Taton, T. A.; Mirkin, C. A.; Letsinger, R. L. *Science* **2000**, *289*, 1757–1760.
(14) Love, J. C.; Estroff, L. A.; Kriebel, J. K.; Nuzzo, R. G.; Whitesides, G. M. *Chem. Rev.* **2005**, *105*, 1103–1169.
(15) Cao, Y. C.; Jin, R.; Mirkin, C. A. *Science* **2002**, *297*, 1536–1540.
(16) Park, S.-J.; Taton, T. A.; Mirkin, C. A. *Science* **2002**, *295*, 1503–1506.

JA102271R